Available online at www.sciencedirect.com
SCIENCE DIRECT®
International Journal of Heat and Fluid Flow 24 (2003) 747–761
International Journal of HEAT AND FLUID FLOW
www.elsevier.com/locate/ijhff

Pressure losses in the laminar flow of shear-thinning power-law fluids across a sudden axisymmetric expansion

F.T. Pinho [a,*], P.J. Oliveira [b], J.P. Miranda [c]

[a] Centro de Estudos de Fenómenos de Transporte, DEMEGI, Faculdade de Engenharia, Universidade do Porto, Rua Dr. Roberto Frias, 4200-465 Porto, Portugal
[b] Departamento de Eng. Electromecânica, Universidade da Beira Interior, Rua Marquês D'Ávila e Bolama, 6201-001 Covilhã, Portugal
[c] Instituto Politécnico de Bragança, Escola Superior de Tecnologia e Gestão, Campus de Santa Apolónia, 5301-857 Bragança, Portugal

Received 29 July 2002; accepted 8 May 2003

Abstract

A numerical investigation was carried out to study the laminar non-Newtonian flow through an axisymmetric sudden expansion having a diameter ratio of 1 to 2.6. The fluids were inelastic and shear thinning with a viscosity obeying the power law model. The recirculation length and strength and, most importantly, the local loss coefficient C_I were quantified as a function of the inlet pipe Reynolds number and shear-thinning intensity. When using the generalised Reynolds number introduced by Metzner and Reed [AIChEJ 1 (1955) 434] (Re_{gen}), at low Reynolds numbers C_I increased by more than 100% when n varied from 1.0 to 0.2, whereas C_I decreased by more than 50% at high Reynolds numbers. However, this feature was shown to be related to the definition of the Reynolds number. A correlation between C_I, Re_{gen} and n is presented at the end.
© 2003 Elsevier Inc. All rights reserved.

Keywords: Sudden expansion; Pressure loss; Shear thinning; Recirculation length

1. Introduction

Sudden expansion flows occur frequently in many industrial applications and bring together geometric simplicity with a not so simple flow behaviour. They have been extensively investigated in the past for Newtonian fluids both numerically (Habib and Whitelaw, 1982; Macagno and Hung, 1967; Oliveira and Pinho, 1997) and experimentally (Stieglmeier et al., 1989; Khezzar et al., 1985; Back and Roschke, 1972) amongst others, in the laminar and mainly in the turbulent flow regimes.

When the fluids exhibit non-Newtonian characteristics the literature is scarcer. Halmos and Boger (1975) investigated experimentally some mean flow characteristics in a 1:2 sudden expansion in laminar flow and their measurements showed that the length of the recirculation bubble was increased by the shear-thinning intensity. The numerical works of Halmos et al. (1975) and Perera and Walters (1977) reached similar conclusions as far as the role of shear-thinning and elasticity are concerned, although the flow conditions were not the same. Halmos et al. (1975) considered fully developed flow at the inlet of the expansion and their numerical results showed a systematic over-prediction of the recirculation length by 7% relative to the measurements of Halmos and Boger (1975). Perera and Walters (1977) studied the hydrodynamics of an expansion/contraction/expansion duct and their concern was the investigation of elastic effects. They concluded that there were no significant changes of hydrodynamic behaviour between shear-thinning fluids and equivalent Newtonian liquids due to pure viscous effects. The definition of an equivalent Newtonian fluid embedding some of the differences between non-Newtonian and Newtonian fluids, helped to reach this conclusion. On the effect of elasticity, however, Halmos and Boger (1976) observed a reduction in recirculation length when the stress ratio exceeded a critical value and found it to be proportional to the Weissenberg number of the flow. This was attributed to a die swelling type of effect.

* Corresponding author. Tel.: +351-225-081-762; fax: +351-225-081-763.
E-mail addresses: fpinho@fe.up.pt (F.T. Pinho), pjpo@ubi.pt (P.J. Oliveira), jmiranda@ipb.pt (J.P. Miranda).

0142-727X/$ - see front matter © 2003 Elsevier Inc. All rights reserved.
doi:10.1016/S0142-727X(03)00083-3

Nomenclature

C_I	local loss coefficient ($C_I \equiv \Delta p_I / \frac{1}{2}\rho U_1^2$)
ΔC	corrective pressure coefficient
D	pipe diameter
f	Darcy friction factor
h	step height
k	consistency index of viscosity power law
L	length
n	power index of the viscosity power law
p	pressure
Δp	pressure difference
r	radial coordinate
Re_{gen}	generalized Reynolds number, Eq. (17)
Re_{mod}	modified Reynolds number, Eq. (18)
U	bulk velocity, $U = \overline{u}$
x	axial coordinate
x_r	recirculation length ($X_r \equiv x_r/h$)
Y	height of the wedge-shaped computational domain

Greeks

α	profile shape factor for energy ($\alpha = \overline{u^3}/U^3$), Eq. (8)
β	profile shape factor for momentum ($\beta = \overline{u^2}/U^2$), Eq. (9)
μ_a	apparent viscosity
Ψ	Stream function
ρ	fluid density
σ	area ratio
τ	shear stress

Subscripts

c-th	theoretical values corrected for friction, momentum and pressure effects
F	fully developed wall frictional contribution
I	irreversible contribution
max	maximum
$p0$	non-uniform pressure effect
R	reversible contribution
th	standard theoretical value
tot	total
β	momentum effect
01	plane just upstream of the expansion
02	plane just downstream of expansion
1	inlet pipe
2	outlet pipe

Superscripts

– (overbar)	cross-section area average

More recently, Pak et al. (1990) conducted similar experiments and showed the opposing effects of viscoelasticity in the laminar and turbulent regimes: elasticity reduced the recirculation length in the former case but increased its size in the latter. Thus, for laminar flow, their findings confirmed the trends previously reported.

For the turbulent flow of drag reducing fluids, Pak et al. (1990, 1991) presented pressure and mean velocity data measurements in an axisymmetric sudden expansion, but did not report the corresponding turbulent flow field. This motivated recent experimental research in the field by Castro and Pinho (1995), Escudier and Smith (1999) and Pereira and Pinho (2000, 2002), who did not confirm the trends due to fluid elasticity, but this could be because the fluids used were less elastic than those used previously by Pak et al.

Other works on viscoelastic sudden expansion flows at very low Reynolds numbers were by Baloch et al. (1995, 1996) and Missirlis et al. (1998). Baloch et al. (1995) concentrated on assessing three-dimensional effects on large expansion ratio geometries whereas Baloch et al.'s (1996) numerical work used the exponential Phan–Thien-Tanner model for predicting mean flow characteristics. Missirlis et al.'s (1998) work, in contrast, was aimed at developing a numerical method rather than at investigating in detail the expansion flow and their predictions were for the constant viscosity, elastic Upper Convected Maxwell model.

For Bingham and Herschel-Bulkley fluids Vradis and Ötügen (1997) and Hammad et al. (2001) have also conducted numerical experiments, but these works were basically aimed at assessing the effect of yield stress upon kinematic quantities (velocity profiles and recirculation length).

In spite of these efforts not much attention has been devoted to the issue of pressure losses in sudden expansions in a useful way, hence Newtonian correlations are usually used for the purpose of calculating the pumping power in non-Newtonian duct flows. Two exceptions to this state of affairs are noted: the experimental work of Edwards et al. (1985) and the theoretical work of Gupta (1965). The main objective of Edwards et al. (1985) was to experimentally quantify the variation of the irreversible pressure loss coefficient with the Reynolds number for Newtonian and power law fluids. At low Reynolds numbers they reported the inverse law ($C_I = A/Re$) with a coefficient that depended on the expansion ratio but not on the power law index. At intermediate Reynolds numbers ($Re \approx 250$), the irreversible pressure loss coefficient varied linearly with the Reynolds number and above this value it tended to the turbulent flow asymptotic value, regardless of fluid

rheology. The transition from the inverse law to a constant C_I value was very smooth and quick. Unfortunately, by not accounting for the differences between the true and fully developed friction losses in the upstream and downstream pipes, their coefficients are not exact and are not directly comparable to those reported in this paper.

For laminar Newtonian pipe sudden expansion flows, Oliveira and Pinho (1997) and Oliveira et al. (1998) have clearly demonstrated that the local loss coefficient differs by a large amount from the standard expressions found in reference books and manuals (Crane, 1999; Hooper, 1988), with the differences increasing as the Reynolds number is reduced. These differences are bound to be more severe with non-Newtonian fluids and this work is aimed at quantifying them numerically in a systematic way, and also at reporting other hydrodynamic characteristics of the flow in axisymmetric sudden expansions. The theoretical work of Gupta (1965) was a first contribution to this aim but no account was given to viscous effects, therefore his expression, which is equivalent to an uncorrected C_{RI} in our work, is in large error to the true local loss coefficient, as will be seen.

This sets the stage for the present work: a numerical investigation of sudden expansion flows of purely viscous non-Newtonian fluids without yield stress, aimed at obtaining the variation of the local loss coefficient as a function of the Reynolds number and the degree of shear thinning. As a subsidiary result, the recirculation length and the strength of the eddy are also quantified but over a more limited range of conditions.

The next section presents the problem and is followed by an outline of the numerical procedure, the specifications of the calculation domain and the boundary conditions. This is followed by a brief outline of the theory underlying the determination of the local loss coefficients, an assessment of the uncertainty of the calculations and the presentation and discussion of results. The paper ends with a summary of the main conclusions and the presentation of a useful correlation for C_I for engineering practice.

2. Basic equations and the numerical method

Fig. 1 shows schematically the axisymmetric sudden expansion and the control volume used. There is a long pipe of length L_1 and diameter D_1 upstream of the sudden expansion to ensure a fully developed inlet flow. Downstream of the sudden expansion plane the pipe is also sufficiently long (length L_2, diameter D_2) for the flow to redevelop again.

The calculations are aimed at obtaining various global flow quantities as a function of the Reynolds number (Re) and shear-thinning intensity (n). Those quantities are the recirculation length ($X_R \equiv x_r/h$, $h = (D_2 - D_1)/2$), the maximum value of the stream function in the recirculation region (ψ_C) and the local pressure loss coefficient C_I. To this aim it is necessary to solve numerically the continuity equation (Eq. (1)) and the momentum equation (Eq. (2)), where the rheological constitutive equation is that of a purely viscous generalized Newtonian fluid.

$$\frac{\partial u_i}{\partial x_i} = 0 \tag{1}$$

$$\rho\left[\frac{\partial u_i}{\partial t} + \frac{\partial (u_i u_j)}{\partial x_j}\right] = -\frac{\partial p}{\partial x_i} + \frac{\partial}{\partial x_j}\left[\eta(\dot\gamma)\left(\frac{\partial u_i}{\partial x_j} + \frac{\partial u_j}{\partial x_i}\right)\right] \tag{2}$$

In Eq. (2) $\eta(\dot\gamma)$ is the viscosity function given by the power law model

$$\eta(\dot\gamma) = k\dot\gamma^{n-1} \tag{3}$$

where the shear rate $\dot\gamma$ is related to the second invariant of the rate of deformation tensor (D_{ij}) by

$$\dot\gamma = \sqrt{2D_{ij}D_{ij}} \quad \text{with } D_{ij} = \frac{1}{2}\left(\frac{\partial u_i}{\partial x_j} + \frac{\partial u_j}{\partial x_i}\right) \tag{4}$$

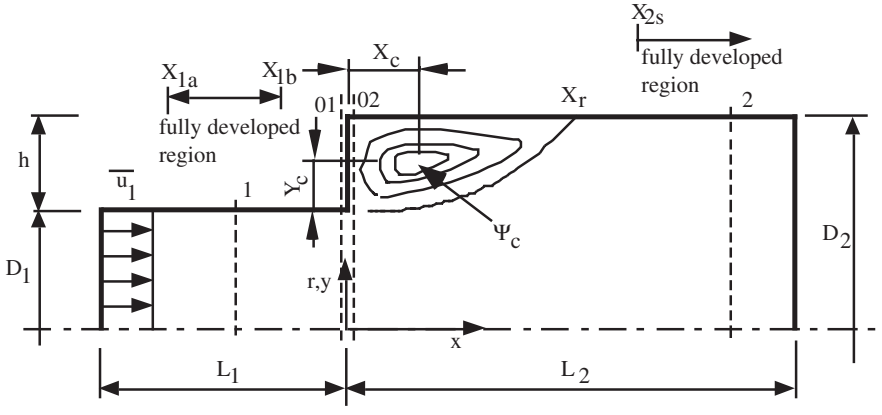

Fig. 1. Schematic representation of sudden expansion geometry and control volume.

Eqs. (1)–(4) were solved with a general-purpose CFD code developed by Oliveira (1992), which is based on the finite-volume method applied to non-staggered meshes. Extension to deal with non-Newtonian fluids of variable viscosity is straightforward, being similar to the handling of Reynolds-averaged equations for turbulent Newtonian flows when using the concept of turbulent viscosity. Therefore, a Newtonian code simply has to be modified to include a variable viscosity function and the turbulence model must be switched off. The boundary conditions imposed for the sudden expansion flow problem are clear from Fig. 1: at inlet ($x = -L_1$), a uniform velocity profile is given, in agreement with the desired Reynolds number; at outlet ($x = +L_2$), zero axial gradients ($\partial/\partial x \equiv 0$) are assumed to all variables (except pressure); at walls ($r = D_1/2$, $r = D_2/2$ and $x = 0$), no slip conditions are imposed. The differencing schemes adopted are all formally second order: central differences for the diffusion terms and second order upwind for the convection terms. The pressure–velocity coupling was dealt with a time-marching form of the SIMPLEC algorithm (Issa and Oliveira, 1994), the sets of linear equations were solved with conjugate gradient methods (preconditioned biconjugate solver for u and v, symmetric conjugate solver for p), and all the calculations were performed with a Pentium/133 MHz computer with 128 Mb RAM.

3. Theory

The main quantity of interest in this work is the irreversible pressure loss coefficient (C_I) which is defined as

$$C_I \equiv \frac{\Delta p_I}{\frac{1}{2}\rho U_1^2} = \frac{\Delta p - \Delta p_R - \Delta p_F}{\frac{1}{2}\rho U_1^2} \tag{5}$$

where the overall pressure drop between planes 1 and 2 in Fig. 1 is $\Delta p = p_1 - p_2$ and may be decomposed into irreversible (I), reversible (R) and fully developed (F) frictional pressure drops: $\Delta p = \Delta p_I + \Delta p_R + \Delta p_F$ as determined from an integral energy balance applied to the control volume of the figure. The reversible pressure drop is given in Eq. (6), the fully developed frictional pressure loss is the sum defined in Eq. (7),

$$\Delta p_R = \frac{1}{2}\rho(\alpha_1 U_1^2 - \alpha_2 U_2^2) \tag{6}$$

$$\Delta p_F = f_1 \frac{L_1}{D_1}\frac{\rho U_1^2}{2} + f_2 \frac{L_2}{D_2}\frac{\rho U_2^2}{2} \tag{7}$$

and so the irreversible pressure drop Δp_I includes not only the effect of the sudden expansion itself but also a friction effect, because the actual friction loss between stations 1 and 2 (cf. Fig. 1) is different from the corresponding fully developed friction losses. In this work, the theory underlying the calculation of the loss coefficient for Newtonian fluids presented by Oliveira and Pinho (1997) is adopted. That theory is independent of the fluid viscosity law except for the profile shape factors for energy $\alpha = \overline{u^3}/U^3$ and momentum $\beta = \overline{u^2}/U^2$, where the overbar denotes average over the cross-section of the pipes. For power law fluids with power index n those two factors are given by

$$\alpha = \frac{3(3n+1)^2}{(2n+1)(5n+3)} \tag{8}$$

$$\beta = \frac{3n+1}{2n+1} \tag{9}$$

for fully developed conditions.

Oliveira and Pinho (1997) have demonstrated that the true pressure loss for Newtonian fluids (C_I) differed significantly from the standard theory coefficient ($C_{I\text{–th}}$) found in manuals and textbooks and derived a 1-D theory to explain the difference. The theory is independent of the law of variation of viscosity provided the fluid is purely viscous, thus for generalized Newtonian fluids the final relationship for correcting the standard coefficient $C_{I\text{–th}}$, and yielding $C_{Ic\text{–th}}$ (c-th for corrected theory), is also given by

$$C_{Ic\text{–th}} = C_{I\text{–th}} - \{\Delta C_F + \Delta C_\beta - \Delta C_{p0}\} \tag{10}$$

The various corrective terms account for different effects: ΔC_F accounts for the differences between the true and fully developed frictional losses in the upstream and downstream pipes and is given by

$$\Delta C_F = \frac{L_1}{D_1}\left(f_1 - 4\frac{\overline{\tau_{w1}}}{\frac{1}{2}\rho U_1^2}\right) + \frac{L_2}{D_2}\left(f_2\sigma^2 - 4\frac{\overline{\tau_{w2}}}{\frac{1}{2}\rho U_1^2}\right) \tag{11}$$

ΔC_β accounts for the effect of radial distortions in the inlet axial velocity profile and is given by

$$\Delta C_\beta = 2(1-\sigma)(\beta_1 - \beta_{01}) \tag{12}$$

and finally ΔC_{p0} takes into account non-uniformities of the pressure at the expansion measured by

$$\Delta C_{p0} = (1-\sigma)(\overline{C}_{p01} - \overline{C}_{p02}) \tag{13}$$

The standard theoretical loss coefficient was then found to be given by

$$C_{I\text{–th}} = \alpha_1\left(1 - \frac{\alpha_2}{\alpha_1}\sigma^2\right) - 2\beta_1\sigma\left(1 - \frac{\beta_2}{\beta_1}\sigma\right) \tag{14}$$

which simplifies to Eq. (15) for conditions of fully developed flow at inlet and outlet.

$$C_{I\text{–th}} = \alpha(1-\sigma^2) - 2\beta\sigma(1-\sigma) \tag{15}$$

Clearly, this expression reduces to the well-known Borda–Carnot local loss coefficient, equal to $(1-\sigma)^2$ when $\alpha = \beta = 1$ (uniform velocity profile), and the first term on the right-hand-side is the "reversible" pressure recovery readily obtained from application of Bernoulli's equation.

The true irreversible pressure loss coefficient (C_I) is directly determined from the computed pressure variations along the centreline, after adequate curve fitting of the data and discounting the fully developed pressure from the total pressure decrease (see details in Oliveira and Pinho, 1997).

4. Grid testing and validation

The solution of a 2-D axisymmetric flow with a full 3-D code based on non-orthogonal coordinates and Cartesian velocity components requires the use of a computational domain with the shape of a wedge of triangular cross section. This is usual practice and the required corrections are those described in the previous work (Oliveira and Pinho, 1997). The present work follows on the same steps and the following must be done in order for the results to be comparable.

First, the bulk velocity in the calculations (U) must be modified so that the mass flow rate in the triangular wedge duct is the same as in the circular pipe. The friction factor is calculated using

$$f = \frac{4\tau_w}{\frac{1}{2}\rho U^2}\frac{D}{2Y} \tag{16}$$

where D is the diameter of the pipe and Y is the height of the triangular wedge. This result corresponds to that of the flow in a circular pipe at $Re = \rho VD/\mu_a$, with V representing the bulk velocity in the circular pipe at the same flow rate and μ_a an apparent viscosity.

For these power law fluids the Reynolds number used is the generalized Reynolds number of Metzner and Reed (1955) given in Eq. (17), here defined in terms of upstream pipe characteristics and where k and n are the consistency and power indices of the Ostwald de Waele power law (Eq. (3)).

$$Re_{\text{gen}} = \frac{\rho D_1^n U_1^{2-n}}{k} 8\left(\frac{n}{6n+2}\right)^n \tag{17}$$

We start by presenting results of fully developed flow in a straight pipe using a uniform mesh with 20 radial cells. Predicted and theoretical friction factors for Newtonian and power law fluids compare well in the plots of Fig. 2. Differences cannot be detected in the Figure but they increase with shear-thinning: for $n = 1$ the error does not exceed 0.31%, but grows to 0.5% and 0.75% for $n = 0.4$ and $n = 0.2$, respectively.

Radial profiles of the normalised axial velocity for different values of the power index are plotted in Fig. 3 for a generalized Reynolds number of 200. The agreement is as good as for the friction factor, and there is again a deterioration with shear-thinning: differences between the predicted and the theoretical velocity profile are within 0.2% for $n = 0.8$ and $n = 1.0$, 0.4% for $n = 0.4$ and $n = 0.6$, and increase to values of the order of 1% for $n = 0.2$. This deterioration for $n = 0.2$ is a consequence of the extreme stiffness of the matrices of the discretised momentum equations since the viscosities tend to very large values in the core of the duct whenever $\dot{\gamma}$ goes to zero (cf. Eq. (3)) (Pinho, 2001). For highly shear-thinning fluids, the results can be improved if the convergence tolerance is further reduced, at the cost of extremely time consuming calculations (all calculations here were converged to a normalised L_1 residual of 1×10^{-5}). An alternative approach to improve numerical

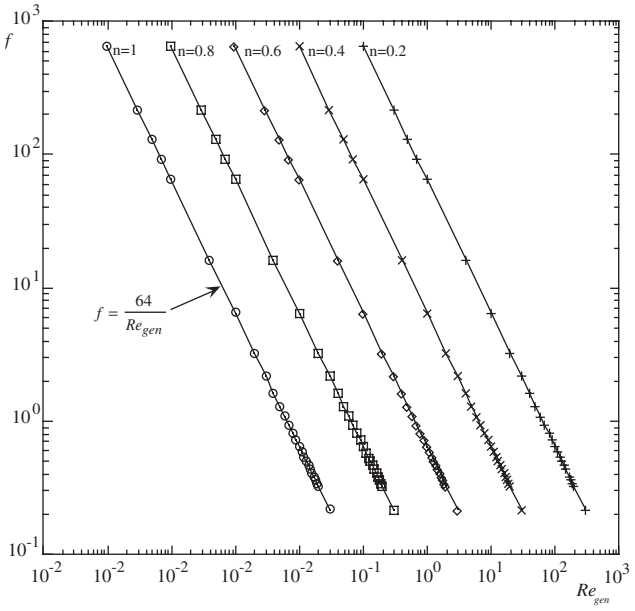

Fig. 2. Comparison between the theoretical (lines, $f = 64/Re_{\text{gen}}$) and calculated (symbols) friction factors at the inlet pipe as a function of the power law index.

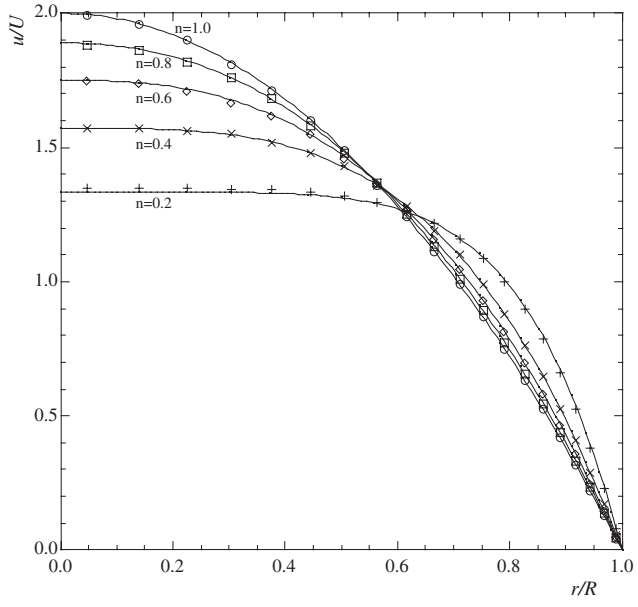

Fig. 3. Radial profiles of the normalised axial velocity for power law fluids: symbols: calculations; lines: theory.

convergence is to use a Carreau model for viscosity instead of the power law, hence avoiding the singular behaviour as $\dot{\gamma} \to 0$, with unnoticeable consequences on the overall results.

Due to the deterioration of the accuracy of results with shear-thinning intensity, a thorough assessment of the errors had to be done in the 1:2.6 diameter ratio sudden expansion of Oliveira and Pinho (1997) using three meshes with different degrees of refinement. Mesh M2S was that used for Newtonian fluids by Oliveira and Pinho (1997), who found that the key factor in the grid was the smallest mesh spacing in the vicinity of the re-entrant corner which should at least be of about 0.10 mm (in non-dimensional form $\delta_x/(D_1/2) \approx 1/47$ and $\delta_x/(D_2 - D_1)/2 \approx 1/76$) for the uncertainty in the calculation not to exceed 0.2%. Mesh M1S was coarser by a factor of 2, whereas mesh 3S was finer also by a factor of 2. The characteristics of these three meshes are presented in Table 1. In each case, three mesh-generating blocks have been used: the first block was located in the inlet pipe, the second block was in the outlet pipe, immediately downstream of the inlet pipe, and the third block was also located in the outlet pipe, but downstream of the expansion wall. These meshes (denoted *S* from "standard") were used for the simulations at low Reynolds numbers ($Re_{gen} \leqslant 50$) and high values of n ($n = 0.4$ to 1.0); for $Re_{gen} > 50$ and $n = 0.2$ the meshes in Table 2 had to be used, having larger inlet and outlet pipes (denoted "large", *L*). These longer pipes were required for complete flow development when the Reynolds number was increased and/or the power index was decreased. In addition, accurate determination of the local loss coefficient requires precise values of the friction coefficient in fully developed flow, which are obtained by the curve fitting procedure described by Oliveira and Pinho (1997), and that entails longer development sections.

Predictions of the local loss coefficient C_I and the normalized recirculation length X_R based on these three meshes enable evaluation of extrapolated values by the technique of Richardson extrapolation to the limit (e.g. Ferziger, 1981). Such results are presented in Tables 3–5, and give an adequate picture of the accuracy of the present sudden expansion calculations. Since all subsequent calculations in Section 5 were carried out with the medium mesh, the relative error ε for any given quantity A is calculated as $\varepsilon = (A_{M2} - A_{ext})/A_{ext} \times 100$, where the subscript ext indicates the extrapolated value and *M2* refers to values obtained with mesh M2 (M2S or M2L, as appropriate).

The uncertainties in C_I are fairly constant with n not exceeding 1% at high Reynolds number, but can go up to 2% for very low Reynolds numbers. For the normalized recirculation length the deterioration in accuracy is more intense and errors can be as high as 10% at low Reynolds numbers, and 5% at high Reynolds numbers, with very shear-thinning fluids. For the location of the eddy center (X_C) the uncertainties are larger than for the recirculation length, whereas for the

Table 1
Characteristics of the meshes for the standard geometry ($L_1/D_1 = 20$, $L_2/D_2 = 20$)

Mesh	Block I				Block II				Block III			
	N_x	N_y	f_x	f_y	N_x	N_y	f_x	f_y	N_x	N_y	f_x	f_y
M1S	20	10	0.7517	0.8530	35	10	1.1909	0.8530	35	16	1.1909	1.1025
M2S	40	20	0.8670	0.9236	70	20	1.0913	0.9236	70	32	1.0913	1.0500
M3S	80	40	0.9311	0.9610	140	40	1.0447	0.9610	140	64	1.0447	1.0247

Table 2
Characteristics of the meshes for the long geometry ($L_1/D_1 = 100$, $L_2/D_2 = 100$)

Mesh	Block I				Block II				Block III			
	N_x	N_y	f_x	f_y	N_x	N_y	f_x	f_y	N_x	N_y	f_x	f_y
M1L	25	10	0.7455	0.8530	45	10	1.1875	0.8530	45	16	1.1875	1.1025
M2L	50	20	0.8841	0.9236	90	20	1.095	0.9236	90	32	1.095	1.0500
M3L	100	40	0.9292	0.9610	180	40	1.0439	0.9610	180	64	1.0439	1.0247

Table 3
Estimation of uncertainty in the calculation of C_I and X_r for fluids with $n = 1$

Re_{g1}	C_I					X_r				
	M1	M2	M3	Ri	ε^a [%]	M1	M2	M3	Ri	ε^a [%]
0.1	165.107	166.689	167.380	168.004	+0.78	0.4583	0.4799	0.4856	0.4876	−1.57
4	4.270	4.291	4.299	4.305	−0.33	0.6682	0.6815	0.6856	0.6871	−0.82
60	1.305	1.307	1.309	1.311	−0.36	6.141	6.114	6.104	6.100	+0.23

[a] Relative error for mesh M2 values.

Table 4
Estimation of uncertainty in the calculation of C_I and X_r for fluids with $n = 0.8$

Re_{g1}	C_I					X_r				
	M1	M2	M3	Ri	ε^a [%]	M1	M2	M3	Ri	ε^a [%]
0.1	196.518	196.743	197.176	197.823	−0.55	0.3319	0.3565	0.3643	0.3672	−2.92
4	5.032	5.012	5.013	5.021	−0.19	0.4647	0.4845	0.4909	0.4933	−1.79
60	1.191	1.191	1.192	1.194	−0.22	3.950	4.252	4.261	4.251	+0.02

[a] Relative error for mesh M2 values.

Table 5
Estimation of uncertainty in the calculation of C_I and X_r for fluids with $n = 0.4$

Re_{g1}	C_I					X_r				
	M1	M2	M3	Ri	ε^a [%]	M1	M2	M3	Ri	ε^a [%]
0.1	288.785	286.771	285.254	283.397	+1.19	0.1331	0.1517	0.1595	0.1663	−8.78
4	7.355	7.160	7.127	7.137	+0.32	0.1671	0.1758	0.1858	0.1996	−11.9
60	0.904	0.904	0.901	0.896	+0.89	1.658	1.667	1.685	1.712	−2.62

[a] Relative error for mesh M2 values.

eddy strength (Ψ_C) they are of the same order as those of X_R.

Improved predictions of X_R, X_C and Ψ_C would have required the use of mesh M3 on a shorter calculation domain for the low Reynolds number simulations, and possibly a tighter convergence residual, but the simulations would have taken significantly longer running times. This was not attempted as the main objective of the work was the determination of the local loss coefficient for which mesh M2 gives adequate accuracy. For these reasons, the predicted values of X_r in Section 5 are given for a more limited range of Re than those of C_I.

For the Newtonian fluid we note that the recirculation length, the maximum value of the stream function and the location of the eddy centre matched the experimental data of Macagno and Hung (1967) and Back and Roschke (1972), as well as the correlations of Badekas and Knight (1992) and Scott et al. (1986) which were derived on the basis of experimental and numerical data. Predictions of the pressure loss coefficient C_I, as well as the various corrections of Eq. (10), were found to be within 0.1% of the values obtained by Oliveira and Pinho (1997).

Comparison with experimental data from the literature for non-Newtonian fluids is significantly more difficult because there are few works where the fluids behaved as purely viscous fluids. One such case is that reported by Halmos et al. (1975) and Halmos and Boger (1975) who have performed both numerical and experimental work. Unfortunately, the experimental x_r data of Halmos and Boger are plotted in a way that does not allow data retrieval for direct comparison, and thus one must rely on some indirect assessment. Even such indirect comparisons with the numerical results of Halmos and Boger (1975) must be carried out carefully, as will be shown below. These authors were only able to attain converged solutions for power law fluids with $n \geqslant 0.65$, due to limitations of their numerical method.

In Fig. 4, the agreement between the numerical results of Halmos et al. (1975) and our predictions for Newtonian fluids is excellent, provided the fully developed inlet profile is imposed right at the expansion plane following those authors, rather than considering the more realistic situation of allowing the flow to develop along an upstream pipe. A modified Reynolds number definition is used

$$Re_{\mathrm{mod}} = \frac{\rho D_1^n U_1^{2-n}}{k} \tag{18}$$

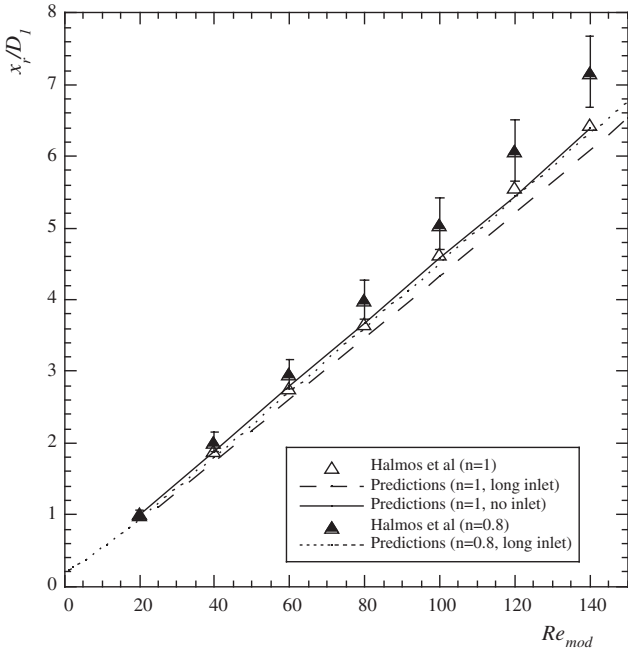

Fig. 4. Comparison with Halmos et al.'s (1975) predictions of recirculation bubble length as a function of inlet Reynolds number for a 1:2 sudden expansion flow of power law fluids. 7% error bars on Halmos et al. ($n = 0.8$) data. "No inlet" refers to a fully developed velocity profile imposed right at the expansion plane.

which differs from the generalised Reynolds number by a factor of $8(n/(6n+2))^n$.

For power law fluids our predictions are always lower than those of Halmos et al. (1975), although to a lesser extent when the inlet fully developed velocity profile is set at the expansion plane, as done by Halmos et al. Note also that the predictions of Halmos et al. were always consistently higher by 7% than the experimental values measured by Halmos and Boger (1975).

Different inlet conditions, mesh resolutions and machine accuracy explain the discrepancies observed in Fig. 4. Whereas Halmos et al. (1975) imposed a fully developed profile immediately upstream of the expansion, the present calculations are more realistic since the flow is allowed to develop in a long upstream pipe, as in Halmos and Boger's experiments. As demonstrated by Oliveira and Pinho (1997) for Newtonian fluids, different shapes of the inlet velocity have an influence on the predicted recirculation bubble length, as well as on the local loss coefficient. This is confirmed in Fig. 4 which includes our predictions for $n = 1$ with the parabolic velocity profile set at the expansion plane (no inlet), showing a close match with the predictions of Halmos et al. (1975). This influence of inlet condition is expected to increase as the power index decreases, since the shear rate at the wall increases and the flow becomes more sensitive to small changes in profile shape. Note that the distortion of the velocity profile at the inlet to the expansion gives a flatter profile which results in a reduction of the recirculation length in agreement with the discrepancies in Fig. 4 (a constant velocity at inlet leads to a shorter recirculation bubble).

Another cause for discrepancies were the limitations of computer power in the early works. Halmos et al. (1975) used a very coarse uniform mesh with 10 cells in the radial direction, giving a normalised cell spacing of 0.1 (see also Halmos (1973) for more details on their computations and numerical method), while the mesh here was non-uniform and the normalised cell spacing in the shear layer was as low as 0.021. For non-Newtonian shear-thinning fluids the issue of mesh refinement is even more relevant. The mesh must be refined in regions of high shear rate, to properly resolve the variations in apparent viscosity and thus accurately calculate the velocity field. Hence, it is important to use a very fine mesh especially near the walls and in the shear layer downstream of the expansion plane. Last, but not least, Halmos used a CDC 3200 machine which in those days had an accuracy of approximately 5 to 6 decimal places so increasing significantly round off errors (Halmos, 1994). Bearing in mind these aspects, it is not difficult to account for the observed differences.

A final reason for the discrepancy between predictions and experiments concerns the fluid behaviour. Whereas the fluid model used is a power law, the real fluid has a low shear rate constant viscosity and, as mentioned by Halmos and Boger (1975), this could also explain why the measured recirculation lengths are shorter than the calculated values.

5. Main results and discussion

Any of the quantities of interest in this investigation depends on the expansion ratio, the inlet condition, a Reynolds number and other non-dimensional numbers taking into account the fluid rheology. For the power law fluids under investigation and taking as example the recirculation length, such functional relationship can be written as

$$\frac{x_r}{h} = f\left(\frac{D_2}{D_1},\ \frac{\rho D_1 U_1}{\mu_{\text{char}}},\ \text{inlet condition}\right) \tag{19}$$

A question that arises with non-Newtonian fluid flows concerns the definition of Reynolds number. For pipe flow there is general agreement on the use of either the wall viscosity, especially under the turbulent regime, or an apparent viscosity based on the definition of the generalised Reynolds number (Re_{gen}) of Metzner and Reed (1955). The latter forces the collapse of the friction factor versus Re_{gen} data for power law fluids onto a single curve.

Research on turbulent sudden expansion and backward facing step flows with Newtonian fluids (Adams et al., 1984) have shown that a better collapse of data can be obtained with the use of the step height (h), instead of the upstream diameter (D_1), to define the normalised recirculation length and the Reynolds number. However, since the flow regime here is laminar and the main focus is on the local loss coefficient, it is advantageous to base the Reynolds number on the inlet pipe characteristics and use the generalised Reynolds number definition of Eq. (17) because fully developed friction factors are traditionally based on such definition.

The present calculations are for an expansion with a diameter ratio of 1 to 2.6 and for Reynolds numbers from ≈ 0.1 up to order 200. The upper limit was set based on information from the literature for Newtonian fluids, which shows instabilities arising in expansion flows when the inlet Reynolds number is in the range of a few hundred. For a 1:2.6 diameter ratio expansion, Back and Roschke (1972) report the existence of wave motions in the shear layer between the pipe jet and the recirculating bubble at Reynolds numbers of around 250. These waves propagate downstream and are amplified at higher Reynolds numbers defining a new flow regime. Similar instabilities were reported by Iribarne et al. (1972) in a 1:2 expansion and at a Reynolds number of 350 a new transition leads to the onset of tangential motion. These investigators also concluded that a fully developed inlet profile delays the transition to higher Reynolds numbers.

5.1. Size and intensity of the recirculation

We start by presenting results for the recirculation bubble, namely the variation of its normalised length and intensity with the generalised Reynolds number and power law index, in Figs. 5 and 6 respectively. The variation of $X_r = x_r/h$ with the Reynolds number is linear at high Reynolds numbers but asymptotes to a constant value at creeping flow conditions. This asymptotic value of X_r decreases with shear-thinning.

For Newtonian fluids, the X_r data compares well with the results from the literature (Oliveira and Pinho, 1997; Macagno and Hung, 1967; Badekas and Knight, 1992; Scott et al., 1986 among others). At very low Reynolds numbers the calculated value of X_r of around 0.47 agrees well with the results reported in the literature and it is important to notice that, for creeping flow conditions, the flow around a sudden contraction is identical to that around a sudden expansion. For a 1:2 sudden expansion Macagno and Hung (1967) calculated $X_r = 0.54$, and for a 1:2.26 expansion Monnet et al. (1982) measured $X_r = 0.476$. For sudden contractions Nguyen and Boger (1979) found a constant x_r/D_2 between 0.17 and 0.18, for diameter ratios above than 4. Subsequent work (for instance Coates et al., 1992) has confirmed $x_r/D_2 = 0.17$ which is equivalent to $X_r = 0.46$ for a 1:4 expansion.

For $n = 0.2$, X_r also asymptotes to a constant value at low Reynolds number, but these predictions are not shown in the figure due to their lower accuracy (see Section 4).

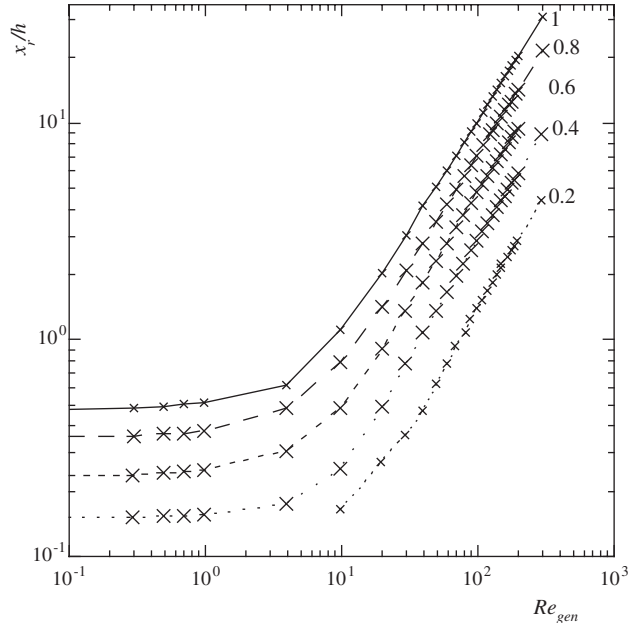

Fig. 5. Variation of the recirculation length with the power law index and the inlet Reynolds number for power law fluids for a 1:2.6 expansion.

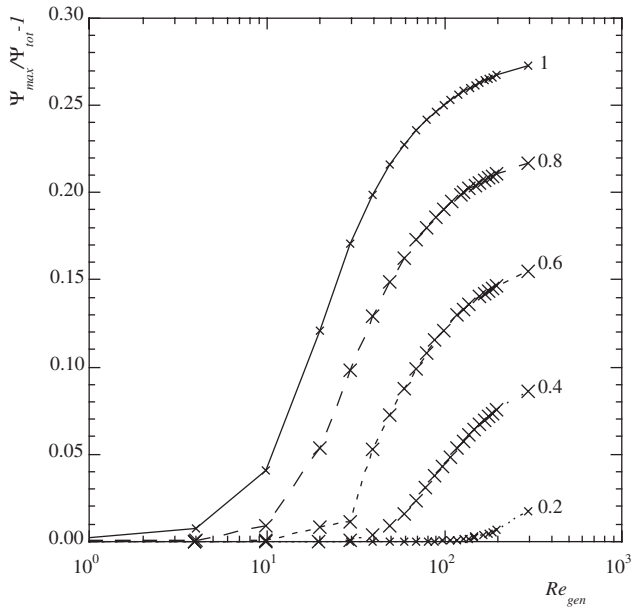

Fig. 6. Variation of the eddy strength with the power index and inlet Reynolds number for power law fluids in a 2.6 expansion.

The intensity of the recirculation bubble Ψ_c shown in Fig. 6 was determined from the predicted stream function field Ψ, which is calculated from integration of the flow rate, starting at the pipe axis.

The figure shows how the eddy strength decreases with increased shear thinning, because the local viscosity inside the eddy tends to increase due to the low shear rates there. This is also observed in the contour plots of the viscosity shown in Fig. 7. The quantity plotted is the ratio of the viscosity to the apparent viscosity in the upstream pipe. It is clear that high viscosities appear within the recirculating region and in the center of the redeveloping downstream flow. This increased viscosity inside the recirculation bubble is also responsible for the reduction of its size as seen in Fig. 5. Nevertheless, it is noticed that at low Reynolds numbers the eddy has a small but finite recirculation intensity.

5.2. Irreversible loss coefficient

The variation of the local loss coefficient is given in Fig. 8 as a function of the shear-thinning intensity, for the two definitions of Reynolds numbers, Re_{gen} (Fig. 8a) and Re_{mod} (Fig. 8b), defined respectively in Eqs. (17) and (18). Likewise the results for a Newtonian fluid of Oliveira and Pinho (1997), two regions of behaviour are observed: at high Reynolds numbers (any $Re_{gen} > 50$) the loss coefficient C_I tends to a constant value typical of inertia dominated flow, whereas at low Reynolds numbers the flow field is totally dominated by viscous effects and C_I varies with Re following an inverse law. In between these two regions there is a transitional behaviour. Some of the data plotted in this figure are listed in

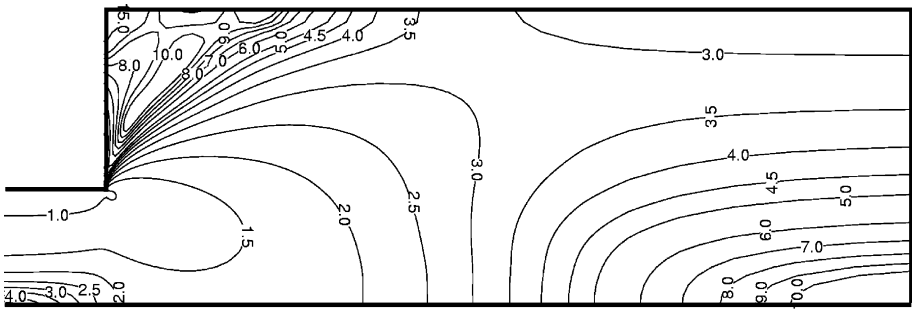

Fig. 7. Contours of μ/μ_a in the vicinity of the expansion for a moderate shear thinning fluid ($n = 0.6$) at $Re_{gen} = 19.69$.

Tables 6–10 together with the various corrections embodied in Eq. (10). These data are useful for benchmarking and for future comparison and extensions of this work. Not perceptible from the figure is the existence of a slight minimum of C_I at an intermediate Reynolds number, a feature previously reported by Oliveira and Pinho (1997) and Oliveira et al. (1998) for Newtonian fluids. The difference between this minimum C_I and the asymptotic C_I value at high Re is rather small and decreases with shear thinning.

A finding common to Newtonian fluid flow (Oliveira and Pinho, 1997) is that the predicted local loss coefficient for power law fluids is very different from the value of the literature ($C_{I\text{–th}}$, Eq. (15)) and this discrepancy increases with shear thinning: at high Reynolds number, where the standard theoretical value is numerically and physically more correct, $C_{I\text{–th}}$ differs from the true value of C_I by 24% for a Newtonian fluid, the difference growing to 37% for $n = 0.6$ and 64% for $n = 0.2$. At first instance the opposite trend would appear more logical, because the velocity profiles tend to become flatter with shear thinning and thus the conditions used to derive $C_{I\text{–th}}$ are closer satisfied. However, the viscous effects associated with n far outweigh the effect of the velocity profile shape.

When the generalised Reynolds number is adopted (Fig. 8a), the effect of shear thinning is opposite at high and low Reynolds numbers: at high Reynolds numbers the loss coefficient decreases with shear thinning, whereas at low Reynolds numbers shear thinning increases the pressure loss. It should be clear, however, that the trends of the C_I variation with Re seen in Fig. 8(a) are, to a large extent, influenced by the definition adopted for the Reynolds number itself. When the same C_I data are plotted as a function of the modified Reynolds number as in Fig. 8b then a reduction of the local loss coefficient with shear thinning is observed throughout the whole range.

The behaviour at high Reynolds numbers is basically related to the shape of the mean velocity profile and its deformation in the vicinity of the sudden expansion. For a highly shear-thinning fluid the velocity profile is closer to a plug shape and any further deformation is inhibited, as discussed hereafter. First, the distortion in the upstream velocity profile on approaching the expansion is such that it tends to flatten the profile shape. Since the

Table 6
Predicted (C_I), corrections and corrected theoretical loss coefficient ($C_{Ic\text{–th}}$) in the 1:2.6 sudden expansion for $n = 1$ ($C_{I\text{–th}} = 1.620$)

Re_{gen}	C_I	β_{01}	ΔC_β	ΔC_{F1}	ΔC_{F2}	ΔC_{p0}	$C_{Ic\text{–th}}$ (Eq. (10))	Error [%][a]
0.0989	166.7	1.219	0.1948	−25.62	11.84	156.2	171.4	+2.8
0.2966	55.57	1.220	0.1931	−8.478	3.983	50.89	56.82	+2.2
0.4944	33.34	1.221	0.1914	−5.088	2.412	30.03	34.13	+2.4
0.9887	16.71	1.224	0.1863	−2.484	1.236	14.39	17.07	+2.2
3.955	4.291	1.241	0.1573	−0.5635	0.3658	2.715	4.375	+1.9
9.887	2.001	1.266	0.1147	−0.1954	0.2255	0.5588	2.034	+1.6
19.775	1.465	1.287	0.0789	−0.0821	0.2217	0.0799	1.481	+1.1
29.66	1.360	1.297	0.0619	−0.0482	0.2329	−0.0029	1.370	+0.8
39.55	1.325	1.303	0.0517	−0.0331	0.2419	−0.0261	1.333	+0.6
49.44	1.312	1.307	0.0449	−0.0244	0.2473	−0.0335	1.318	+0.5
69.21	1.305	1.312	0.0363	−0.0155	0.2553	−0.0353	1.308	+0.3
98.87	1.306	1.316	0.0278	−0.0100	0.2612	−0.0314	1.309	+0.3
128.5	1.309	1.319	0.0244	−0.0065	0.2648	−0.0272	1.310	+0.1
148.3	1.311	1.321	0.0210	−0.0053	0.2664	−0.0248	1.313	+0.1
168.1	1.313	1.322	0.0193	−0.0047	0.2677	−0.0228	1.315	+0.1
197.8	1.315	1.323	0.0176	−0.0037	0.2691	−0.0202	1.316	+0.1

[a] Error $= (C_{Ic\text{–th}} - C_I)/C_I \times 100$.

Table 7
Predicted (C_I), corrections and corrected theoretical loss coefficient (C_{Ic-th}) in the 1:2.6 sudden expansion for $n = 0.8$ ($C_{I-th} = 1.534$)

Re_{gen}	C_I	β_{01}	ΔC_β	ΔC_{F1}	ΔC_{F2}	ΔC_{p0}	C_{Ic-th} (Eq. (10))	Error [%][a]
0.0987	196.7	1.197	0.1886	−26.75	20.10	167.3	175.3	−10.9
0.2956	65.72	1.198	0.1869	−8.871	6.740	61.62	65.09	−1.0
0.4933	39.34	1.199	0.1852	−5.324	4.067	36.49	39.10	−0.6
0.9865	19.76	1.202	0.1807	−2.623	2.065	17.65	19.56	−1.0
3.946	5.012	1.215	0.1579	−0.6098	0.5732	3.564	4.976	−0.7
9.865	2.191	1.234	0.1249	−0.2157	0.2911	0.8672	2.200	+0.4
19.73	1.435	1.255	0.0898	−0.0892	0.2578	0.1645	1.440	+0.3
29.60	1.275	1.266	0.0710	−0.0512	0.2627	0.0275	1.279	+0.3
39.46	1.222	1.273	0.0591	−0.0345	0.2680	−0.0128	1.228	+0.5
49.33	1.201	1.278	0.0506	−0.0253	0.2766	−0.0275	1.205	+0.3
69.06	1.186	1.284	0.0404	−0.0158	0.2846	−0.0349	1.190	+0.3
98.66	1.184	1.289	0.0318	−0.0096	0.2930	−0.0334	1.185	+0.1
128.2	1.186	1.292	0.0267	−0.0068	0.2978	−0.0298	1.186	+0.01
148.0	1.188	1.294	0.0233	−0.0054	0.2995	−0.0275	1.189	+0.1
167.7	1.189	1.295	0.0216	−0.0044	0.3011	−0.0255	1.190	+0.04
197.3	1.192	1.296	0.0199	−0.0036	0.3029	−0.0229	1.191	−0.02

[a] Error $= (C_{Ic-th} - C_I)/C_I \times 100$.

Table 8
Predicted (C_I), corrections and corrected theoretical loss coefficient (C_{Ic-th}) in the 1:2.6 sudden expansion for $n = 0.6$ ($C_{I-th} = 1.422$)

Re_{gen}	C_I	β_{01}	ΔC_β	ΔC_{F1}	ΔC_{F2}	ΔC_{p0}	C_{Ic-th} (Eq. (10))	Error [%][a]
0.0984	235.2	1.170	0.1750	−26.71	34.73	231.4	224.6	−4.5
0.2953	78.45	1.171	0.1733	−8.869	11.62	76.39	74.89	−4.5
0.4921	46.90	1.171	0.1716	−5.278	6.996	45.39	44.92	−4.2
0.9843	23.46	1.173	0.1699	−2.705	3.495	22.14	22.61	−3.6
3.937	5.902	1.182	0.1546	−0.6189	0.9412	4.742	5.687	−3.6
9.843	2.481	1.196	0.1307	−0.2285	0.4449	1.346	2.420	−2.4
19.69	1.459	1.212	0.1035	−0.0985	0.3173	0.3442	1.443	−1.1
29.53	1.203	1.224	0.0830	−0.0568	0.3001	0.0977	1.192	−0.9
39.37	1.110	1.232	0.0694	−0.0376	0.3018	0.0159	1.104	−0.5
49.21	1.068	1.238	0.0592	−0.0264	0.3070	−0.0154	1.066	−0.1
68.9	1.041	1.245	0.0472	−0.0158	0.3165	−0.0342	1.039	−0.1
98.43	1.032	1.251	0.0353	−0.0095	0.3260	−0.0369	1.033	+0.03
128.0	1.033	1.255	0.0302	−0.0066	0.3319	−0.0343	1.032	−0.1
147.6	1.034	1.257	0.0268	−0.0051	0.3349	−0.0321	1.033	−0.1
167.3	1.035	1.258	0.0234	−0.0046	0.3371	−0.0301	1.035	+0.03
196.9	1.037	1.260	0.0217	−0.0035	0.3393	−0.0273	1.037	−0.05

[a] Error $= (C_{Ic-th} - C_I)/C_I \times 100$.

profiles are already quite flat due to shear thinning, smaller changes are prone to take place. Secondly, flatter velocity profiles produce high viscosities in the core of the pipe and this tends to induce additional resistance to distortions in the velocity and pressure profiles. Hence, as shear thinning increases the modifications of the velocity profile become more localised and tend to occur closer to the wall. This is shown in Fig. 9 where the momentum shape factor at the end of the upstream pipe (β_{01}) is plotted as a function of the generalised Reynolds number and n. In all cases β_{01} is constant at low Re, then it increases tending to an asymptote at large Re. As n decreases, the values of β_{01} are reduced due to flatter velocity profiles, the rise in β_{01} is delayed to higher Reynolds numbers and the differences between the high and low Reynolds number asymptotic values decrease. This is clear evidence of a smaller amount of distortion in the upstream velocity profile.

At low Reynolds numbers, the use of Re_{gen} leads to the misleading trends commented above and seen in Fig. 8a, and for that reason it is better to consider Re_{mod} as the main independent parameter for the physical characterisation of pressure losses in the expansion. However, Re_{gen} will still be employed for the correlation developed in Section 5.3, because it is more practical for the evaluation of pressure losses in piping systems which have historically been based on the generalised Reynolds number. For frictional losses in a straight pipe its use provides a unique expression for $f(f = 64/Re_{gen})$ regardless of the shear-thinning intensity.

Table 9
Predicted (C_I), corrections and corrected theoretical loss coefficient (C_{Ic-th}) in the 1:2.6 sudden expansion for $n = 0.4$ ($C_{I-th} = 1.269$)

Re_{gen}	C_I	β_{01}	ΔC_β	ΔC_{F1}	ΔC_{F2}	ΔC_{p0}	C_{Ic-th} (Eq. (10))	Error [%][a]
0.0982	286.8	1.134	0.1503	−24.82	59.73	294.76	261.0	−9.0
0.2946	95.69	1.134	0.1503	−8.163	19.95	97.59	86.92	−9.0
0.4910	57.20	1.135	0.1486	−4.681	12.00	58.16	51.96	−9.0
0.9821	28.78	1.136	0.1469	−2.346	6.035	28.58	26.02	−9.6
3.928	7.160	1.141	0.1384	−0.5822	1.570	6.433	6.576	−8.1
9.820	2.931	1.148	0.1265	−0.2260	0.6949	2.068	2.742	−6.4
19.64	1.587	1.157	0.1111	−0.1073	0.4231	0.6961	1.539	−3.1
29.46	1.201	1.165	0.0975	−0.0607	0.3600	0.2920	1.165	−3.0
39.28	1.029	1.173	0.0839	−0.407	0.3383	0.1212	1.009	−1.9
49.10	0.947	1.180	0.0719	−0.0287	0.3303	0.0390	0.935	−1.3
68.74	0.874	1.189	0.0566	−0.0162	0.3358	−0.0369	0.856	−2.1
98.21	0.850	1.197	0.0430	−0.0097	0.3463	−0.0436	0.846	−0.4
127.7	0.845	1.202	0.0345	−0.0065	0.3546	−0.0435	0.843	−0.2
147.3	0.844	1.204	0.0310	−0.0049	0.3588	−0.0413	0.843	−0.1
167.0	0.846	1.206	0.0276	−0.0040	0.3621	−0.0391	0.845	−0.1
196.4	0.847	1.208	0.0242	−0.0032	0.3660	−0.0358	0.847	−0.1

[a] Error $= (C_{Ic-th} - C_I)/C_I \times 100$.

Table 10
Predicted (C_I), corrections and corrected theoretical loss coefficient (C_{Ic-th}) in the 1:2.6 sudden expansion for $n = 0.2$ ($C_{I-th} = 1.053$)

Re_{gen}	C_I	β_{01}	ΔC_β	ΔC_{F1}	ΔC_{F2}	ΔC_{p0}	C_{Ic-th} (Eq. (10))	Error [%][a]
0.0980	372.8	1.084	0.1003	−18.20	102.6	391.3	307.8	−17.4
0.2939	124.5	1.084	0.1003	−6.204	33.73	130.4	103.8	−16.6
0.4899	74.53	1.084	0.1003	−3.671	20.25	77.89	62.26	−16.5
0.9798	37.32	1.084	0.1003	−1.839	10.172	38.54	31.16	−16.5
3.919	9.355	1.086	0.0969	−0.4987	2.1381	9.028	7.846	−16.1
9.799	3.766	1.087	0.0952	−0.1970	1.1133	3.181	3.223	−14.4
19.60	1.940	1.088	0.0935	−0.0999	0.6371	1.286	1.708	−12.0
29.40	1.376	1.090	0.0901	−0.0654	0.4835	0.6932	1.238	−10.0
39.19	1.076	1.093	0.0849	−0.0456	0.4101	0.4061	1.010	−6.2
48.99	0.896	1.096	0.0798	−0.0343	0.3598	0.2554	0.903	+0.8
68.59	0.801	1.104	0.0662	−0.0211	0.3441	0.0886	0.752	−6.0
97.98	0.700	1.113	0.0509	−0.0117	0.3338	−0.0041	0.676	−3.4
127.4	0.659	1.119	0.0406	−0.0081	0.3346	−0.0393	0.646	−1.9
147.0	0.645	1.123	0.0355	−0.0065	0.3373	−0.0505	0.636	−1.3
166.6	0.635	1.124	0.0321	−0.0050	0.3404	−0.0560	0.629	−0.9
196.0	0.632	1.127	0.0270	−0.0042	0.3000	−0.0581	0.627	−0.7

[a] Error $= (C_{Ic-th} - C_I)/C_I \times 100$.

The 1-D theory presented in Section 3 explains in a simple way the discrepancies between the calculated C_I and the common expression for C_{I-th}, but it is not aimed at providing an exact correction (C_{Ic-th}) to C_{I-th}. The theory works reasonably well for $n \geqslant 0.6$ but produces errors in excess of 5% for strongly shear-thinning fluids, especially at low Reynolds numbers (for instance, 9% and 17% for $n = 0.4$ and 0.2, see Tables 9 and 10). This loss of accuracy is not caused by lack of mesh refinement, but to incomplete convergence of the numerical calculations. With increased levels of shear-thinning the high viscosities within the recirculating eddy lead to very stiff matrices of the discretized equations, which require tighter convergence criteria for identical accuracy levels, and even the 10^{-5} used here for the normalised L_1-norm of the residuals is not sufficiently low tolerance (Pinho, 2001).

Such low tolerances were not tried because the computing time would grow disproportionately without significant improvement on the predictions of C_I. Note that the local loss coefficient is obtained from the pressure variation along the centreline, while the stiff matrices are related to high viscosities especially in the recirculating region and so will have more impact on the corrections ΔC_{p0} and ΔC_{F2}.

The tables also show well that the most important corrections, ΔC_{F2} (wall friction in outlet pipe) and ΔC_{p0} (non-uniform pressure), increase with shear thinning at low Reynolds numbers. In contrast, ΔC_{F1} (wall friction in inlet pipe) looks fairly independent of n, except for the lowest n. Of the large corrections ΔC_{p0} is the most important, especially at low Reynolds numbers, and grows in importance as n decreases. This is shown in Fig. 10,

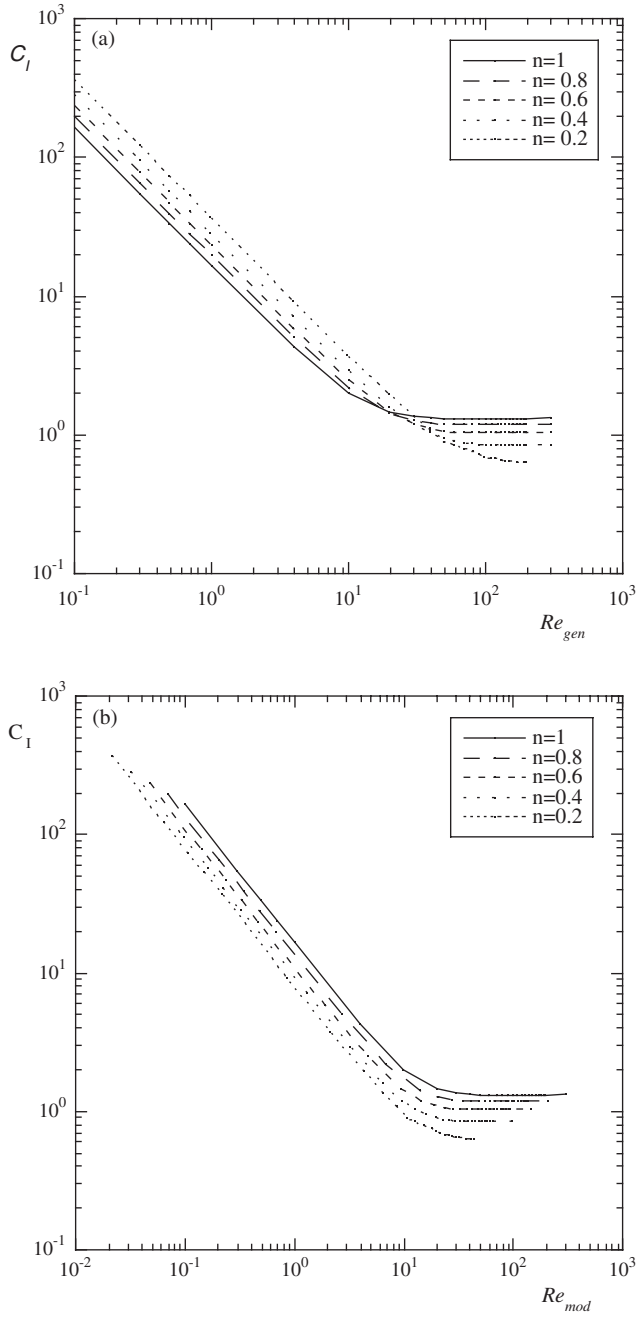

Fig. 8. Variation of the irreversible loss coefficient with power index and Reynolds number in a 1:2.6 expansion: (a) generalised Reynolds number, Eq. (17); (b) modified Reynolds number, Eq. (18).

where the local loss coefficient from the flow simulations, C_I, is compared with corrected-theoretical values (C_{Ic-th}) obtained from Eq. (10) with and without taking into account non-uniformity of pressure fields (ΔC_{p0}). Two values of power law index are considered, $n = 0.8$ (mild shear-thinning, Fig. 10a) and $n = 0.4$ (strong shear thinning, Fig. 10b). Clearly, pressure non-uniformity has an important contribution at low Reynolds numbers, in particular at low n (Fig. 10b). By neglecting its effect, i.e. by assuming a uniform pressure at the exit, the predictions of the corrected-theory show the opposite trend to be the true variation of C_I with Re_{gen}.

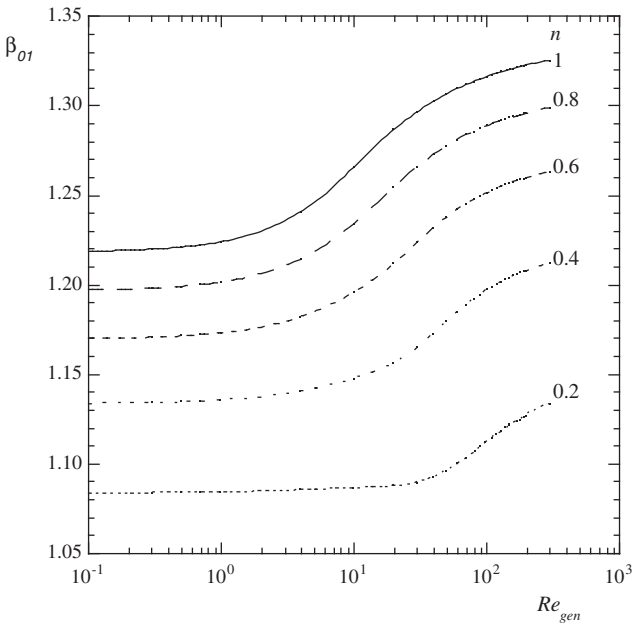

Fig. 9. Variation of the momentum shape factor at the end of the inlet pipe with Reynolds number and power index of power law fluids in a 1:2.6 expansion.

5.3. Correlation for local loss coefficient

More useful from an engineering point of view is a correlation for C_I as a function of Re_{gen} and n. As noted above, Re_{gen} is here preferred to the more physically meaningful Re_{mod}, because it facilitates practical calculations of pressure loss. Following our previous work with Newtonian fluids (Oliveira et al., 1998), the following correlation, obtained by best-fitting techniques, is proposed

$$C_I = \frac{m_1}{Re_{gen}^{m_2}} + m_3 + m_4 \times \log(Re_{gen}) + m_5 \times \log^2(Re_{gen}) \tag{20}$$

where the m_i coefficients are given by the expressions:

$$\begin{aligned} m_1 &= 17.45 - 27.53 \times \log(n) \\ m_2 &= 1 - 0.009n + 0.0027n^2 - 0.010n^3 \\ m_3 &= 0.113 - 1.02n \\ m_4 &= -0.256 + 1.21n + 0.498n^2 \\ m_5 &= 0.124 - 0.0911n - 0.149n^2 - 0.110n^3 \end{aligned} \tag{21}$$

These expressions are to be used only for a sudden axisymmetric expansion with a diameter ratio of 1:2.6 in the range of $0.2 \leqslant n \leqslant 1$ and $0.09 \leqslant Re_{gen} \leqslant 200$. A comparison between the calculated values of C_I and those given by Eq. (20) is shown in Fig. 11. Expression (20)

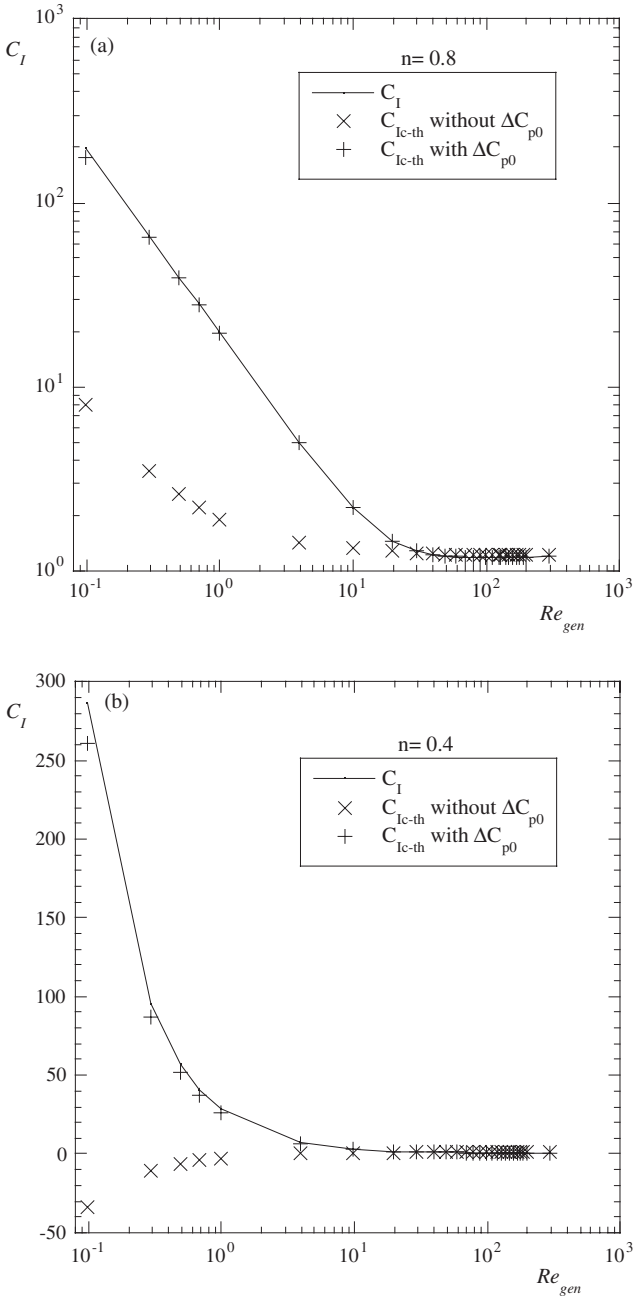

Fig. 10. Effect of n on the pressure correction ΔC_{p0} to C_I: (a) $n = 0.8$, (b) $n = 0.4$.

gives computed values of C_I with accuracies better than 3% at low and high Reynolds numbers and of about 5–6% at intermediate Reynolds numbers.

6. Conclusions

A numerical investigation was carried out to obtain the variation of the local loss coefficient C_I through a 1:2.6 sudden expansion for power law fluids. The effects of shear thinning and Reynolds number were assessed. The variation of the recirculation length and of the eddy strength were also quantified. The main findings were the following:

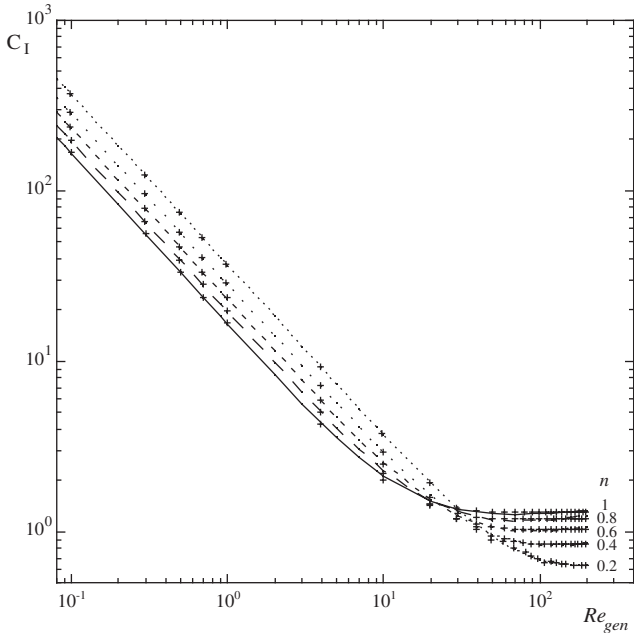

Fig. 11. Comparison between the loss coefficients obtained from the flow simulations (C_I, symbols) and approximate values of C_I from the correlation of Eqs. (20) and (21) (lines).

- The normalized recirculation length decreased with shear thinning, and in all cases two regions of behaviour were observed: a linear variation of X_R at high Reynolds numbers and an asymptotic behaviour as the Reynolds number tended to zero that also depended on n;
- The eddy strength weakened with shear thinning and also exhibited an asymptotic value at low Reynolds numbers. However, at high Reynolds numbers its variation with Re was not linear;
- At low Reynolds numbers the flow was dominated by viscous forces and the local loss coefficient varies inversely with the Reynolds number. When Re_{gen} is employed, the loss coefficient is found to increase with shear-thinning by more than 100% when n decreases from 1 to 0.2;
- At high generalised Reynolds numbers, C_I tends to a constant value which decreases with shear thinning. When employing Re_{gen} a variation in excess of 50% was found when n decreased from 1.0 to 0.2;
- Contrasting with the two previous points, it was found that C_I always decreases monotonically with decreasing n if the modified Reynolds number is adopted as the independent parameter instead of the generalised Reynolds number;
- A correlation was derived for the local loss coefficient, in terms of Re_{gen} and n, to facilitate engineering calculations of pressure losses in piping systems.

Acknowledgements

The authors acknowledge the financial support and facilities provided by the Thermal Engineering Unit (CETERM) of INEGI—Instituto de Engenharia Mecânica e Gestão Industrial in Portugal.

References

Adams, E.W., Johnston, J.P., Eaton, J.K., 1984. Experiments on the structure of turbulent reattaching flows. Report MD-43, Thermosciences Division, Dept. of Mech. Engineering, Stanford University.

Back, L., Roschke, E., 1972. Shear layer regimes and wave instabilities and reattachment lengths downstream of an abrupt circular channel expansion. J. Appl. Mech. September, 677–681.

Badekas, D., Knight, D.D., 1992. Eddy correlations for laminar axisymmetric sudden expansion flows. ASME J. Fluids Eng. 114, 119–121.

Baloch, A., Townsend, P., Webster, M.F., 1995. On two- and three-dimensional expansion flows. Comput. Fluids 24, 863–882.

Baloch, A., Townsend, P., Webster, M.F., 1996. On vortex development in viscoelastic expansion and contraction flows. J. Non-Newt. Fluid Mech. 65, 133–149.

Castro, O.S., Pinho, F.T., 1995. Turbulent expansion flow of low molecular weight shear-thinning solutions. Exp. Fluids 20, 42–55.

Coates, P.J., Armstrong, R.C., Brown, R.A., 1992. Calculation of steady-state viscoelastic flow through axisymmetric contractions with the EEME formulation. J. Non-Newt. Fluid Mech. 42, 141–188.

Crane, 1999. Flow of fluids through valves, fittings and pipe. Technical paper no. 410, Metric edition, Crane Valves Co., Long Beach, CA, USA.

Edwards, M.F., Jadallah, M.S.M., Smith, R., 1985. Head losses in pipe fittings at low Reynolds numbers. Chem. Eng. Res. Des. 63, 43–50.

Escudier, M.P., Smith, S., 1999. Turbulent flow of Newtonian and shear-thinning liquids through a sudden axisymmetric expansion. Exp. Fluids 27, 427–434.

Ferziger, J.H., 1981. Numerical Methods for Engineering Applications. John Wiley & Sons Inc.

Gupta, R.C., 1965. Expansion losses in laminar flows of non-Newtonian fluids. Bull. Calcutta Math. Soc. 57, 117–122.

Habib, M.A., Whitelaw, J.H., 1982. The calculation of turbulent flow in wide-angle diffusers. Numer. Heat Trans. 5, 145.

Halmos, A.L., 1973. The solution of the equations of motion for a non-Newtonian liquid flowing through a sudden expansion using a numerical technique. Report CHER 73-1, Chemical Engineering Department, School of Engineering, Monash University, Australia.

Halmos, A.L., 1994. Personal communication.

Halmos, A.L., Boger, D.V., 1975. The behaviour of a power law fluid flowing through a sudden expansion. Part II. Experimental verification. AIChEJ 21, 550–553.

Halmos, A.L., Boger, D.V., 1976. Flow of viscoelastic polymer solutions through an abrupt 2-to-1 expansion. Trans. Soc. Rheol. 20, 253–264.

Halmos, A.L., Boger, D.V., Cabelli, A., 1975. The behaviour of a power law fluid flowing through a sudden expansion. Part I Numerical solution. AIChEJ 21, 540–549.

Hammad, K.J., Vradis, G.C., Ötügen, M.V., 2001. Laminar flow of a Herschel–Bulkley fluid over an axisymmetric sudden expansion. J. Fluids Eng. 123, 588–594.

Hooper, W.P., 1988. Calculate head loss caused by change in pipe size. Chem. Eng. 95, 89–92.

Iribarne, I., Frantisak, F., Hummel, R.L., Smith, J.W., 1972. An experimental study of instabilities and other flow properties of a laminar pipe jet. AIChEJ 18, 689–698.

Issa, R., Oliveira, P.J., 1994. Numerical prediction of phase separation in two-phase flow through T-junctions. Comput. Fluids 23, 347–372.

Khezzar, L., Whitelaw, J.H., Yianneskis, M., 1985. An experimental study of round sudden expansion flows. Proc. Fifth Symp. on Turb. Shear Flows, Cornell University, pp. 5–25.

Macagno, E.O., Hung, T.K., 1967. Computation and experimental study of a captive annular eddy. J. Fluid Mech. 28, 43–64.

Metzner, A.B., Reed, J.C., 1955. Flow of non-Newtonian fluids—correlation of the laminar, transition and turbulent flow regimes. AIChEJ 1, 434–440.

Missirlis, K.A., Assimacopoulos, D., Mitsoulis, E., 1998. A finite volume approach in the simulation of viscoelastic expansion flows. J. Non-Newt. Fluid Mech. 78, 91–118.

Monnet, P., Menard, C., Sigli, D., 1982. Some new aspects to the slow flow of a viscous fluid through an axisymmetric duct expansion or contraction. II Experimental part. Appl. Sci. Res. 39, 233–248.

Nguyen, H., Boger, D.V., 1979. The kinematics and stability of die entry flows. J. Non-Newt. Fluid Mech. 5, 353–368.

Oliveira, P.J., 1992. Computer modelling of multidimensional multiphase flow and application to T- junctions. PhD thesis, Imperial Collega, University of London.

Oliveira, P.J., Pinho, F.T., 1997. Pressure drop coefficient of laminar Newtonian flow in axisymmetric sudden expansions. Int. J. Heat and Fluid Flow 18, 518–529.

Oliveira, P.J., Pinho, F.T., Schulte, A., 1998. A general correlation for the local loss coefficient in Newtonian axisymmetric sudden expansions. Int. J. Heat Fluid Flow 19, 655–660.

Pak, B., Cho, Y.I., Choi, S.U.S., 1990. Separation and reattachment of non-Newtonian fluid flows in a sudden expansion pipe. J. Non-Newt. Fluid Mech. 37, 175–199.

Pak, B., Cho, Y.I., Choi, S.U.S., 1991. Turbulent hydrodynamic behaviour of a drag-reducing viscoelastic fluid in a sudden expansion pipe. J. Non-Newt. Fluid Mech. 39, 353–373.

Pereira, A.S., Pinho, F.T., 2000. Turbulent characteristics of shear-thinning fluids in recirculating flows. Exp. Fluids 28 (3), 266–278.

Pereira, A.S., Pinho, F.T., 2002. The effect of the expansion ratio on a turbulent non-Newtonian recirculating flow. Exp. Fluids 32, 458–471.

Perera, M.G.N., Walters, K., 1977. Long range memory effects in flows involving abrupt changes in geometry. Part 2: the expansion/contraction/expansion problem. J. Non-Newt. Mech. 2, 191–204.

Pinho, F.T., 2001. The finite-volume method applied to computational rheology: II-Fundamentals for stress-explicit fluids. e-rheo.pt, 1, 63–100. Available from <http://www.dep.uminho.pt/e-rheo.pt/>.

Scott, P., Mirza, F., Vlachopoulos, J., 1986. A finite element analysis of laminar flows through planar and axisymmetric abrupt expansions. Comput. Fluids 14, 423–432.

Stieglmeier, M., Tropea, C., Weiser, N., Nitsche, W., 1989. Experimental investigation of the flow through axisymmetric expansions. J. Fluids Eng. 111, 464–471.

Vradis, G.C., Ötügen, M.V., 1997. The axisymmetric sudden expansion flow of a non-Newtonian viscoplastic fluid. J. Fluids Eng. 119, 193–200.